A Visual Target Representation using Saliency Detection Approach

Shekun Tong*[1], Chunmeng Lu[2]
College of Information Engineering, Jiaozuo University,
Jiaozuo, Henan 454100, P. R. China[1]
College of Artificial Intelligence, Jiaozuo University,
Jiaozuo, Henan, 454100, P. R. China[2]

***Abstract*—The task of saliency detection is to identify the most important and informative part of a scene. Saliency detection is broadly applied to numerous vision problems, including image segmentation, object recognition, image compression, content-based image retrieval, and moving object detection. Existing saliency detection methods suffer a low accuracy rate because of missing components of saliency regions. This study proposes a visual saliency detection method for the target representation to represent targets more accurately. The proposed method consists of five modules. In the first module, the salient region is extracted through manifold ranking on a graph, which incorporates local grouping cues and boundary priors. Secondly, using a region of interest (ROI) algorithm and the subtraction of the salient region from the original image, other parts of the image, either related or nonrelated to the interested target, are segmented. Lastly, those related and non-related regions are classified and distinguished using our proposed algorithm. Experimental result shows that proposed salient region accurately represent the interested target which can be used for object detection and tracking applications.**

Keywords*—Saliency detection; target representation; vision system; object detection

I. Introduction

Saliency detection methods can be categorized into fixation prediction-based and salient object detection methods. Fixation prediction-based methods are strongly related to biological models. Their processes simulate how human fix locate an image. On the other hand, object-oriented approaches generate maps such that salient regions uniformly cover the whole objects [1].

Fixation prediction methods are inspired by biological principles. Itti et al. [2] proposed the seminal bottom-up saliency model derived from the human visual selective attention mechanism. It obtains saliency maps in different feature channels with a center-around operation and combines them linearly. Hou and Zhang [3] presented a saliency model counting for the Fourier envelope and the differential spectral components, called the spectrum residual, to extract salient regions. Garcia-Diaz et al. [4, 5] propose an adaptive approach achieved by decorrelation and contrast normalization. These fixation prediction-based methods usually overemphasize local contrast and difference from the neighborhood. They are more likely to produce spotlight saliency maps with low resolution and high saliency values on the object boundaries.

On the other hand, Achanta et al. [6] compute the saliency likelihood of each pixel based on its color contrast to the entire image. Ming et al. [7] consider the global region contrast concerning image and spatial relationships across the regions to extract a saliency map. In [8], Goferman et al. simultaneously model local low-level clues, global considerations, visual organization rules, and high-level features to highlight salient objects with their contexts. Such methods using local contrast tend to produce higher saliency values near edges instead of uniformly highlighting salient objects.

This paper proposes a new method for saliency detection for target appearance representation in images. It incorporates visual features and spatial information with the guidance of prior saliency knowledge. To provide more accurate visual cues, region descriptors are introduced for image segments by computing two saliency measures, feature distinctiveness, and spatial distribution. In contrast to previous models, which linearly combine basic features for visual cues, we provide nonlinear integration of the features. In addition, by taking the advantage of the prior saliency distribution obtained from a convex hull of salient points, we heighten the contrast of fore- and background [1].

In [9], a bottom-up method is proposed to detect salient regions in images through manifold ranking on a graph, which incorporates local grouping cues and boundary priors. This method adopts a two-stage approach with the background and foreground queries for ranking to generate the saliency maps. This method is taken advantage of node construction for saliency map identification. Fig. 1 shows the node construction in the GMR method.

Although various saliency detection methods are proposed and present promising results, current methods are not feasible and effective when an object is composed of several parts [1]. For example, as shown in Fig. 2, our model fails to detect the wheels since they are discriminated from the main part of the car. Therefore, current saliency detection methods are not effectively able to represent an object, which makes fail object appearance representation in moving object detection systems. Therefore, it is required to investigate an effective approach to deal with this this issue. Fig. 3 shows the saliency fail detection in current methods.

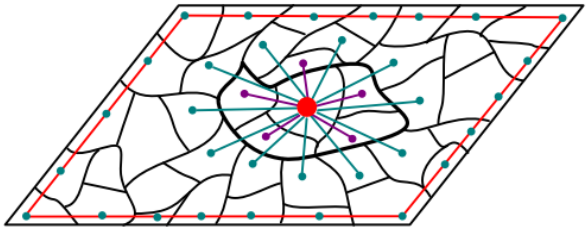

Fig. 1. Nodes construction in GMR [9]

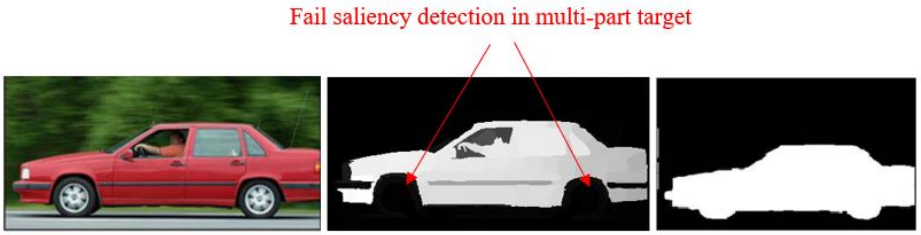

Fig. 2. Fail saliency detection in GMR multi-part saliency detection method. The first image is the original image, the second is the result of saliency map for [9] method and the last image is grand-trouth

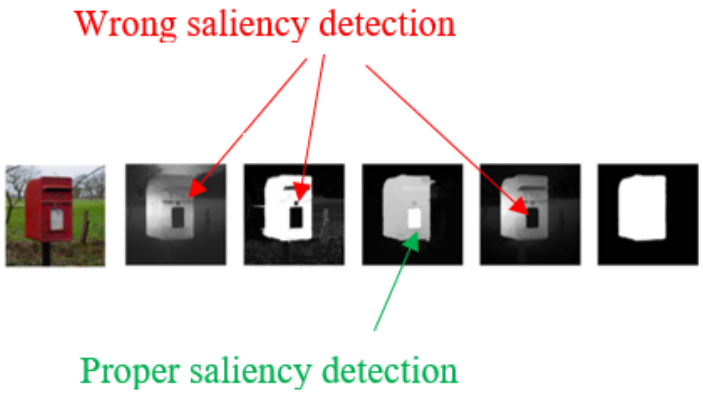

Fig. 3. Wrong and propose saliency detection in different saliency detection methods. The first image is original image, the last image is grand-truth images, and the others from left to right are the saliency map results for LDRCCB [10], SF [11], BS [12], GMR [9]

II. Proposed Method

In dealing with the mentioned problem in the previous step, a saliency detection method is proposed to recognize saliency components for a salient region. This component of saliency recognition aims to represent the accurate region because sometimes they consist of several parts, as shown in Fig. 4, and they are required to recognize. The proposed method is structured by five modules, salient region detection, salient region localization, region of interest extraction, particle region segmentation, and belonging ratio (BRM) measurement. The proposed method for multi-part saliency recognition is shown in Fig. 4. The detail of each step is discussed in the following sub-sections.

A. Salient region Detection

There are numerous region saliency detection methods. This study adopted a graph-based manifold ranking (GMR) method for salient region detection [17]. As reported in [13], the GMR methods presented promising results for salient region detection [9]. The source code of the GMR method is available from the author's website[1]. The source code collects a saliency map of the GMR method. For example, Fig. 5 shows the saliency map (saliency result) using the GMR method. The original image (Fig. 5(a)) was taken from the MSTR-1000 dataset, which is available from the author's website.

B. Salient region Localization

After salient region detection, the localization of the salient region is performed using centroid finding and region size identification [18]. The purpose of localization is to locate the region saliency on the original image. This localization is also used to generate an expanded region to cover different parts of an interested target.

1) Saliency map binarization: To do the localization, the saliency map image is firstly converted to zero 0 and 1 pixels (binarization) using thresholding. The Otsu operator uses for thresholding and binarization. Fig. 6 shows the binarization of the saliency map image.

[1] http://ivrlwww.epfl.ch/supplementary_material/RK_CVPR09

2) Centroid identification: In this step, the centroid of the binary saliency map is identified. The connected component function is used to extract white pixels as a blob. Blob properties are used to recognize the center of the shape. A geometric decomposition algorithm [14, 15] is used to find the centroid identification. In geometric decomposition algorithm, the centroid of a blob figure as X can be computed by decomposing it into certain number of parts as, $X_1, X_1, X_1, \dots, X_n$, therefore, the centroid and area A_i of each part, and then the coordination of C_x and C_y can be computed as equations (1),

$$C_x = \frac{\sum C_{i_x} A_i}{\sum A_i},\ C_y = \frac{\sum C_{i_y} A_i}{\sum A_i} \quad (1)$$

Using above equation, the centroid of salient region can be obtained. The centroid is represented by a coordination that can be used for further process.

3) Region size identification: Bed on the output of the previous step, which was the identified centroid, we can access the centroid coordination of the salient region. Other geometry properties such as the height and width parameters can be specified by this coordination. In this regard, considering $S_{cp}(C_x, C_y)$, where S_{cp} is the center point of salient region, C_x, C_y are the values for X and Y axis. Using the center point and identified height and width, an expanded region with H' and W' are calculated by following equation,

$$W' = W+1/n\ (W) \quad (2)$$

$$H' = H+1/n\ (H)$$

where the W' and H' are the expanded values by the n variable, n is a variable for expanding factor which is set 5 in this experimental. The expanding factor was obtained based on different experiments, assume as n = 6. Fig. 7 shows expanded height and weight of salient region with corresponding center point, *W, H, W' and H'*.

4) Region of interest extraction: The output from the previous step includes information such as expanded region details and salient region center points. This information is used to extract and generate a region of interest (ROI) from a binary saliency map. The extracted region of interest of the binary saliency map is defined as the ROI of the binary saliency map. Moreover, according to ROI, a binary saliency map can be extracted from the saliency map and original image using mapping of the extracted binary saliency map. The extracted new regions from the saliency map and original image are defined as the ROI of the saliency map and the ROI of the original image, respectively. Fig. 8 shows the region of interest extraction for the original, saliency map, and binary saliency map images.

5) Particle region segmentation: In this step, the ROI is segmented into different regions called particles. The purpose of particle region extraction is to extract different regions, including regular and symmetric shapes, from the ROI of the original image. The extracted particles are then transferred to the next step to check whether the particle belonged to the target (the detected salient region) or not. To segment different particles, the following steps are considered; edge segmentation, image enhancement, filling blobs, and applying the proposed shape descriptor. Fig. 9 shows the steps of particle region segmentation.

C. Thresholding and Edge Segmentation

Edges are significant properties of each region. The edges are used to detect region boundaries and segment the region. The segmented region using edges, can be used in more processes, such as region analysis and recognition. In this study, the edges are also used to segment different regions on the ROI of the original image and then generate particles. The particles are defined as different regions that are generated after edge segmentation.

1) Region enhancement and filling blobs: The detected edges from previous steps are contained many disconnected regions. Image enhancement is required to close the regions and remove some noises [19]. Therefore, noise removal [20], mathematical morphology operator [21], lightweight operators including dilation and closing [22], are applied to enhance the result of the edge detection process. Then filling function is applied, to fill the connected blobs in the enhanced image. Fig. 9(c) shows the image result from the image enchantment step.

2) Interested region shape extraction: As shown in Fig. 9(c), the result of image enhancement is still contained many noises, which are required to remove. The noises are involved different types of shapes. To remove these noises, the proposed shape descriptor is applied in this image. Additionally, regular [23] and symmetry [24] regions called interesting shapes (such as wheels) are extracted based on the proposed shape descriptor. With the proposed shape descriptor, the particle regions with regular and symmetry shapes are detected. Since, the final target (the salient region) that we are looking for (such as vehicles) are involved regular components. Fig. 9(d) shows the particle regions result after the interested shape extraction process.

3) Saliency components recognition: As discussed in the previous step, the result of the interest shape extraction step is contained regular and symmetry region shapes, which can be belonged to a salient. The belonged regions define as saliency components. To recognize the saliency components, an algorithm is proposed, which is shown in Table I. In the proposed algorithm, two input images are required. The first input image is a set of particles, including the segmented particles shown in Fig. 10. The other input is a saliency mask. The interior regions of a binary saliency map are filled with this saliency mask. Fig. 11 shows the saliency mask image. The saliency mask is considered because the exterior parts of the salient region are required to be recognized.

The details of proposed algorithm describe as follows.

D. Particle Properties Identification

In this step, the properties of each particle are identified. To do this identification, the edges for particle regions and salient mask are detected, and their region is extracted. The Sobel

edge detector is used for edge segmentation. Fig. 12 shows the edge segmentation of the salient mask. The segmented regions are then integrated into one image. Fig. 13 shows a man-made image, including the integration of a salient mask and some particles regions.

To identify the properties of the particles, the centroid of particle is firstly extracted by taking the particle area and dividing it up into differential areas. The arbitrary shape has an area denoted by *A*. Differential area *dA* that exists some distance *x* and *y* from the origin. The total area is denoted as $\int dA$, which is the first moment of area in each direction from the following Eq. [16]:

$$Q_x = \int_A y\, dA \qquad (3)$$

$$Q_y = \int_A x\, dA$$

The first moment of area is the integral of a length over an area. It is important because it helps us to locate the centroid of the particle. According to the obtained area, the centroid is defined as the "average *x* (or *y*) position of the area"

$$\bar{x} = \frac{Q_y}{A} = \frac{\sum_i \overline{x_i} \overline{A_i}}{\sum_i \overline{A_i}} \qquad (4)$$

$$\bar{y} = \frac{Q_x}{A} = \frac{\sum_i \overline{y_i} \overline{A_i}}{\sum_i \overline{A_i}}$$

Fig. 5 to 15 shows the centroid of the particles using calculation of centroid moments. Using the identified center point, diameter for particle is identified, as shown in Fig. 14.

E. Particle Mask Generation

In this step, a mask is generated according to the shape of the particle inspired from [25]. The purpose of this mask is to determine the range for exploring the area. The exploring area (ExA) is a search range to check whether the particle belongs to the target (salient region) or not. The diameter of the mask depends on particle diameter. It calculates by $D_{mask} = 2*D_{particle}$. Fig. 15 shows the generated particle masks. Furthermore, Fig. 16 shows *ExA* on integrated salient and particles image.

F. Confluence Lines (CL) Generation

Confluence lines (CL) are the lines to find intersection points in different regions. These regions are the particles and the salient region. The *CL* lines are started from the particle center point and end up on the mask. Therefore, it is required to identify the endpoints on the mask to draw these lines. Having the area value of the mask to find the endpoint on the mask or particle is required. The area of the particle mask is considered that can be calculated using Eq. (3).

$$A = \int_0^{\theta} \int_0^{r} dS = \int_0^{\theta} \int_0^{r} \tilde{r} d\tilde{r} d\tilde{\theta} = \int_0^{\theta} \frac{1}{2} r^2 d\tilde{\theta} = \frac{r^2 \theta}{2} \qquad (5)$$

where θ is denoted as an angle between two individual points on the mask region, the radius of the mask, *S* is the region mask, and *A* is the area of the mask. Using the identified area, a mask can be divided into equal sectors. In this regard, several sectors and angles between sectors, are required. The equation is used to address the angle between each sector.

$$\varphi = {}^{2\pi}/_{n} \qquad (6)$$

where n is number of sectors, and θ denotes the angle between CL lines (sectors). According to our experiment, with 20 sectors, we can get promising results. Therefore, the mask contains 20 points (since there are 20 equal sectors on a mask). These points are considered endpoints for *CL* lines in which the angle between the CL lines is as, $\theta = {}^{\pi}/_{10}$. The angle between each pair CL is 18. Fig.17 shows a circle division demonstration inspired by trigonometry constants on real radicals[2]. Fig. 18 illustrates the sectors and confluence lines (CL) in a mask.

G. Particle and Salient Region Distance Measurement

Using the CL lines, the intersection points from the salient region and particles with CL can be extracted. The points form a salient region, and particles are collected; and composed of a pair of two points used for distance measurement. Fig. 19 shows the point on the salient region as P_s and particles as P_p. Euclidean distance (Equation (5)) is used for distance measurement. Then, Fig. 20 shows the result of Euclidean distance for distance measurement between *Ps* and P_p.

$$D_i = \sqrt{\sum_{i=1}^{n} (P_s - P_p)^2} \qquad (7)$$

where, the P_p and P_s are defined as,

$P_p\ (x_i, y_j) \rightarrow$ intersection point for CL and particle, and

$P_s\ (x_{i'}, y_{j'}) \rightarrow$ intersection point for CL and salient region

The obtained distances for each pair of P_s and P_p called D_i are compared. The purpose of this comparison is to identify a number of equal lines and non-lines distances. For identification number of equal and equal distances, we consider conditions as shown in Eq. (6),

$$For\ each\ D_i\ and\ (D_i - 1), if \begin{cases} D_i - (D_{ps} - 1) > \varepsilon \rightarrow N_{eql} = N_{eql} + 1 \\ D_i - (D_{ps} - 1) < \varepsilon \rightarrow N_{non-eql} = N_{non-eql} + 1 \end{cases} \qquad (8)$$

H. Possession Ratio Measurement

In this step, a ratio is introduced to decide whether the particle is belonged to the silent region (target) or not. The ratio is called the possession ratio (or belonging ratio) (μ_{BR}). Eq. (7) is defined in this study to measure the μ_{BR} for each particle. A condition rule then is defined to decide the particle is belonged, which is based on a threshold denoted as δ.

$$\mu_{BR} = 1/n\left(\sum_{i=1}^{n} N_{eq}\right) \qquad (9)$$

where N_{eq} is a counter variable to count the equal distances and n number of lines. Based on obtained value from Eq. (7), a condition defines as shown in Eq. (10), to decide whether the particle is belonged to the target (salient region) or not as,

$$\begin{cases} \mu_{BR} = 1 \quad then \quad P_i \leftarrow T \\ \mu_{BR} > \delta \ and\ \mu < \delta + 0.1 \quad then \quad P_i \leftarrow T \\ \mu_{BR} < \delta \quad then \quad P_i \leftarrow N \end{cases} \qquad (10)$$

According to calculated μ_{BR} and asses the condition, the particle is labeled as True (*T*) or Negative (*N*). Lastly,

[2]https://commons.wikimedia.org/wiki/File:Unit_circle_angles_color.svg

according to *T* and *N* labels, the corresponding particles are recognized as the saliency components.

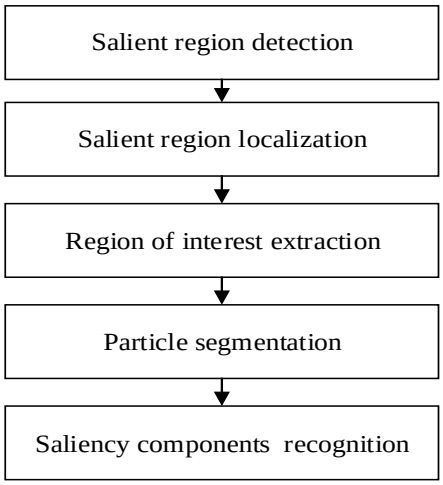

Fig. 4. The proposed method for multi-parts saliency recognition

(a)

(b)

Fig. 5. The saliency map from GMR method, (a): original image, (b): saliency map

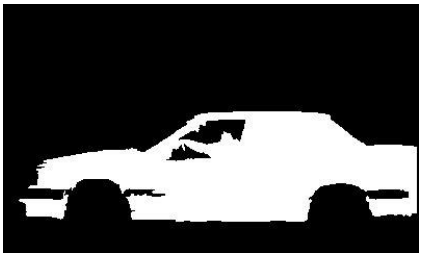

Fig. 6. Binarization of saliency map

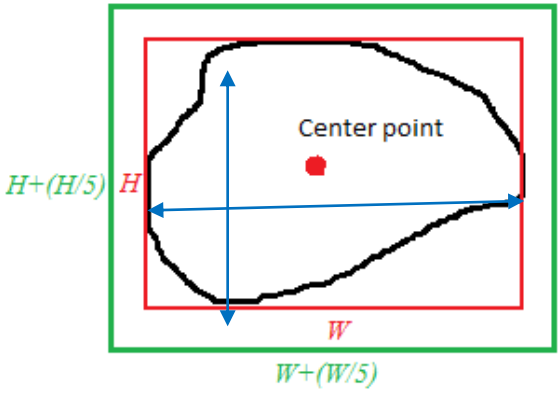

Fig. 7. Expanded height and weight of salient region with corresponding center point

(a) (b) (c)

Fig. 8. Salient region extraction, (a): ROI of binary saliency map, (b): ROI of saliency map (c): ROI of original image

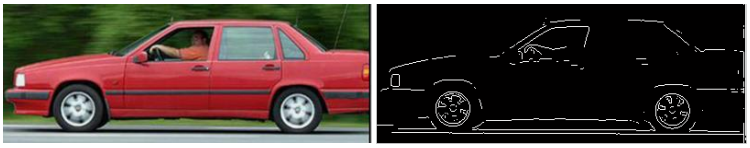

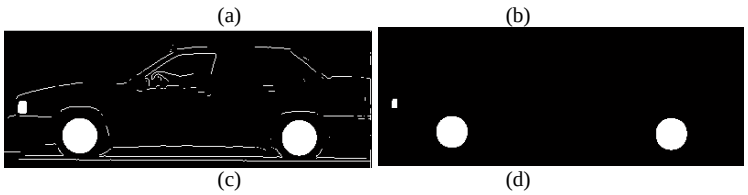

Fig. 9. Particle region segmentation. (a): extracted salient region from orginal image, (b): threasholding and edge segemnetion, (c): region enhancement and filling blobs, and (d): Interested region shape extraction

Fig. 10. A set of particles

Fig. 11. A saliency mask image

TABLE I. COMPONENTS SALIENCY RECOGNITION

Saliency Components Detection Algorithm
Input: A set of particles and salient mask.
Extract the edges for all regions and identify the particle properties such as centroid called as P_c and diameter as P_d,
Particle mask generation with these parameters: Diameter: $2P_d$, *Origin*: particle center (P_c)
Generate confluence lines finder *(CL)* form P_c to confluence the mask circumference (length of lines are equal to 2 P_d)
Measure the distance between points on particle to concern point on salient region touch, using Equation (2).
Count number of equal lines using Equation (3)
Measure the belonging ratio using Equation (4) and identify the particle is belonged to target or not.
Output: a saliency map with its related parts

Fig. 12. Edge segmentation of salient region

Fig. 13. Integration of edge particles and salient region

Fig. 14. Diameter of particles

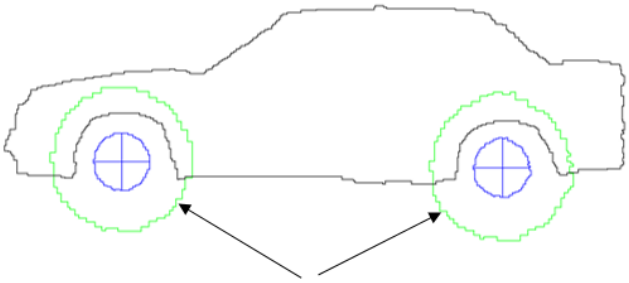

Fig. 15. Generated mask of particles

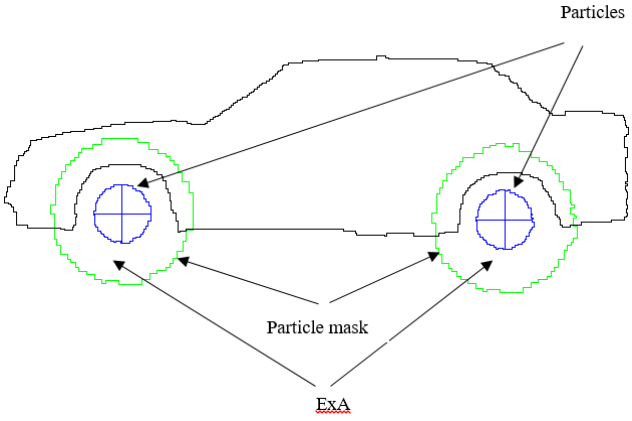

Fig. 16. Exploring area integrated of salient and particles image

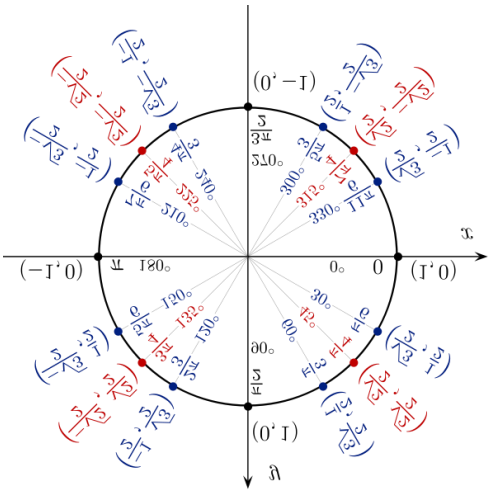

Fig. 17. Circle division into some sectors with angle between CL lines

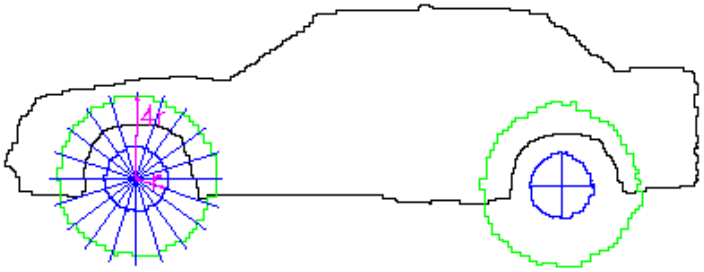

Fig. 18. Sectors and confluence lines (CL) in the mask

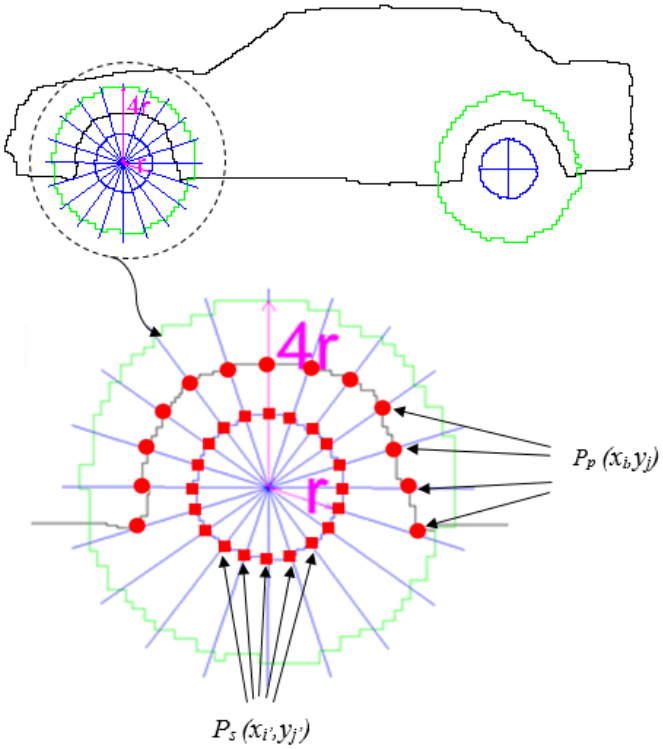

Fig. 19. Points on salient regions and particles

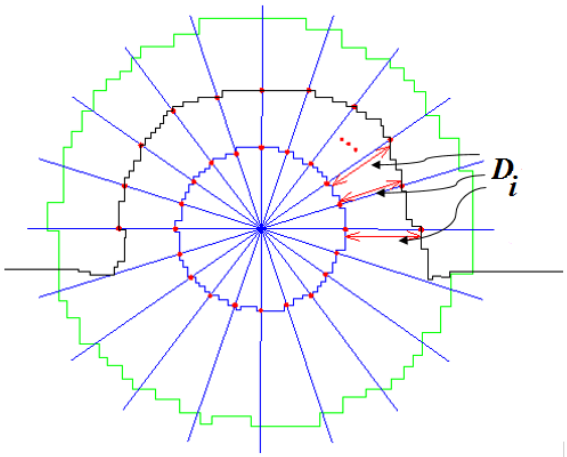

Fig. 20. Distance between salient region ponies and particle points

III. EXPERIMENTAL RESULTS

1In this section, experimental results are presented for the proposed saliency detection method. The proposed method consists of five steps, salient region detection, salient region localization, region of interest extraction, particle segmentation, and multi-part saliency recognition. The salient region detects using the GMR method for an input image. The detected salient region localizes, and the region extract corresponding salient region, is extracted using region of interest extraction. The localization and region of extraction are integrated into one process, because, they are roughly related to each other. The extracted target segments using the segmentation process as explained earlier consist of, an extracted salient region from the original image, there holding and edge segmentation, filling blobs, and shape recognition. Fig. 21 shows the segmentation process for the salient particle segmentation step.

In the last step of the method, associated particles to the salient region detect using the proposed multi-part saline detection. For these steps, segmented particles (as shown in Fig. 21(a)) from particle segmentation steps are evaluated to check whether they belong to the detected salient region or not. This belonging assessment is based on checking distance measurement between the out-bounding of the segmented particle region and binary salient mask. Finally, those segmented particles belong to salient region are added to the saliency map as shown in Fig. 22(c).

According to the proposed saliency detection method, some image results are illustrated as shown in Fig. 23.

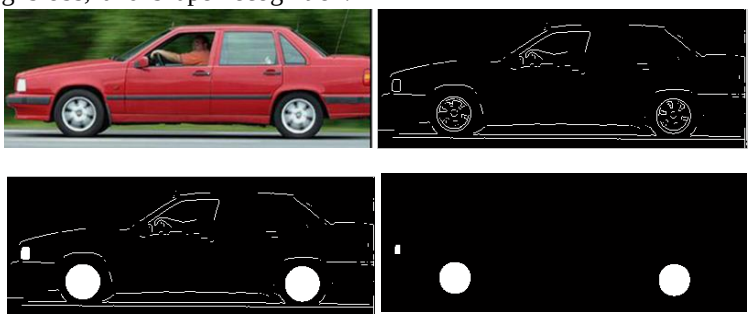

Fig. 21. Particle region segmentation. (a): extracted salient region from original image, (b): thresholding and edge segmentation, (c): filling blobs, and (d): regular shape recognition

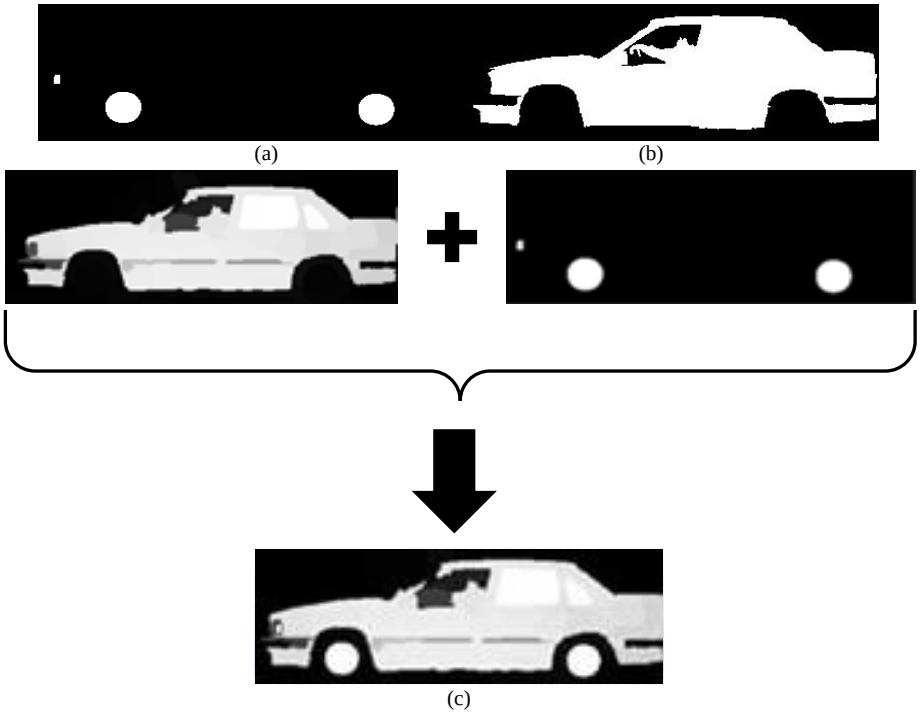

Fig. 22. Multi-part saliency recognition step. (a) segmented particles, (b) binary salient mask

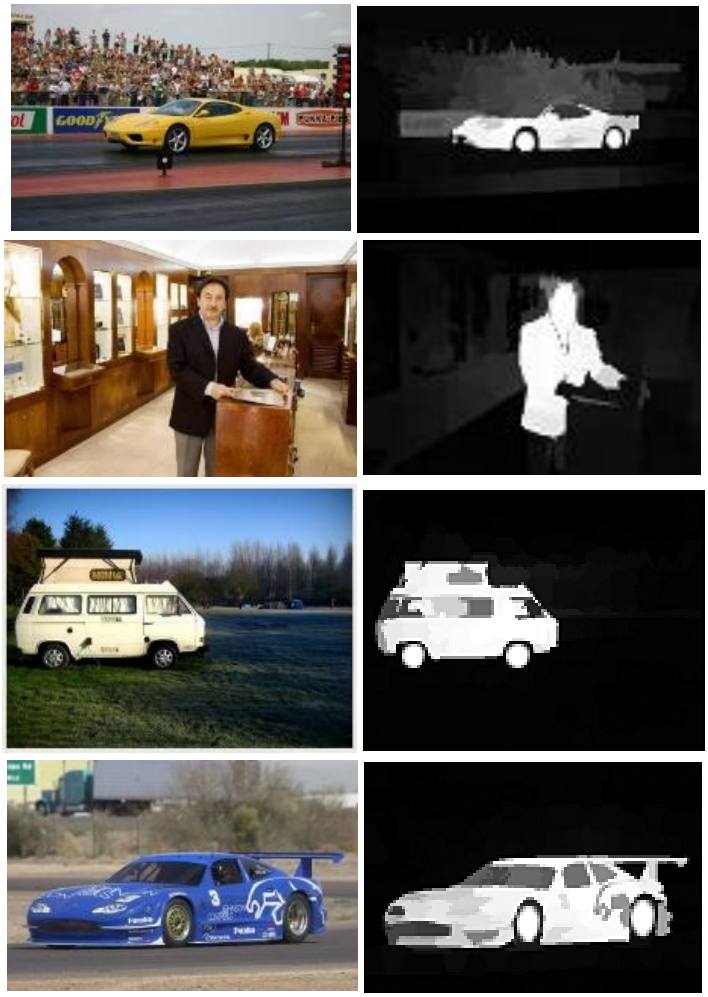

Original image The proposed method

Fig. 23. Experimental result for the proposed saliency detection method

IV. CONCLUSION

In this study a new saliency detection method is proposed based on component saliency recognition for a salient region. This component of saliency recognition aims to represent the salient region more accurately because sometimes the salient regions involve several parts. To deal with component saliency recognition for a salient region, the proposed method is structured by five modules, salient region detection, salient region localization, region of interest extraction, particle region segmentation, and possession ratio measurement. In brief, the proposed method is first applied to a graph-based manifold ranking (GMR) method for salient region detection in an image. The detected salient region is localized using centroid finding and region size identification. The localized region is then extracted and called ROI. In ROI, some processes are performed to segment different regions and generate the particles. The BRM is the main module in our saliency detection method. Finally, as experimental results show, the proposed components' saliency recognition for a salient region can represent accurately and efficiently the target appearance representation. For directions of future study, modern advanced methods such as deep learning frameworks can be explored for further improvement of object representation in visual tracking applications. Moreover, the proposed method can be extended for real time applications.

REFERENCES

[1] Wang, W., et al., Visual saliency detection based on region descriptors and prior knowledge. Signal Processing: Image Communication, 2014. 29(3): pp. 424-433.

[2] Itti, L., C. Koch, and E. Niebur, A model of saliency-based visual attention for rapid scene analysis. IEEE Transactions on Pattern Analysis & Machine Intelligence, 1998(11): pp. 1254-1259.

[3] Hou, X. and L. Zhang. Saliency detection: A spectral residual approach. in Computer Vision and Pattern Recognition, 2007. CVPR'07. IEEE Conference on. 2007. IEEE.

[4] Garcia-Diaz, A., et al., Saliency from hierarchical adaptation through decorrelation and variance normalization. Image and Vision Computing, 2012. 30(1): pp. 51-64.

[5] Garcia-Diaz, A., et al., On the relationship between optical variability, visual saliency, and eye fixations: A computational approach. Journal of vision, 2012. 12(6): pp. 17.

[6] Achanta, R., et al., Salient region detection and segmentation, in Computer Vision Systems. 2008, Springer. pp. 66-75.

[7] Ming-Ming, C., et al. Global contrast based salient region detection. in Computer Vision and Pattern Recognition (CVPR), 2011 IEEE Conference on. 2011.

[8] Goferman, S., L. Zelnik-Manor, and A. Tal, Context-aware saliency detection. Pattern Analysis and Machine Intelligence, IEEE Transactions on, 2012. 34(10): pp. 1915-1926.

[9] Yang, C., et al. Saliency detection via graph-based manifold ranking. in Computer Vision and Pattern Recognition (CVPR), 2013 IEEE Conference on. 2013. IEEE.

[10] Schauerte, B. and R. Stiefelhagen. How the distribution of salient objects in images influences salient object detection. in Image Processing (ICIP), 2013 20th IEEE International Conference on. 2013. IEEE.

[11] Perazzi, F., et al. Saliency filters: Contrast based filtering for salient region detection. in Computer Vision and Pattern Recognition (CVPR), 2012 IEEE Conference on. 2012. IEEE.

[12] Xie, Y., H. Lu, and M.-H. Yang, Bayesian saliency via low and mid level cues. Image Processing, IEEE Transactions on, 2013. 22(5): pp. 1689-1698.

[13] Ali Borji, M.M.C., Huaizu Jiang and Jia Li, Salient Object Detection: A Benchmark IEEE TRANSACTIONS ON IMAGE PROCESSING, 2015.

[14] Chu, M.T. and R.E. Funderlic, The Centroid Decomposition: Relationships between Discrete Variational Decompositions and SVDs. SIAM J. Matrix Anal. Appl., 2001. 23(4): pp. 1025-1044.

[15] Sideway. Centroid by Geometric Decomposition. 2012; Available from: http://output.to/sideway/default.asp?qno=120600007.

[16] Boston, U.o. Centroid and Area Moments. 2013; Available from: http://www.bu.edu/moss/mechanics-of-materials-bending-normal-stress/.

[17] Ullah I, Jian M, Hussain S, Guo J, Yu H, Wang X, Yin Y. A brief survey of visual saliency detection. Multimedia Tools and Applications. 2020. 34605-45.

[18] Liu Y, Xu Z, Ye W, Zhang Z, Weng S, Chang CC, Tang H. Image neural style transfer with preserving the salient regions. IEEE Access. 2019. 40027-37.

[19] Deeba F, Bui FM, Wahid KA. Computer-aided polyp detection based on image enhancement and saliency-based selection. Biomedical signal processing and control. 2020. 101530.

[20] Jiang B, Lu Y, Lu G, Zhang D. Real noise image adjustment networks for saliency-aware stylistic color retouch. Knowledge-Based Systems. 2022.

[21] Chen B, Cheng Y, Zhang W, Mei G. Investigation on enhanced mathematical morphological operators for bearing fault feature extraction. ISA transactions. 2022. 440-59.

[22] Hu M, Yang J, Ling N, Liu Y, Fan J. Lightweight single image deraining algorithm incorporating visual saliency. IET Image Processing. 2022. 16(12). 3190-200.

[23] Zhu L, Ling H, Wu J, Deng H, Liu J. Saliency pattern detection by ranking structured trees. In Proceedings of the IEEE International Conference on Computer Vision. 2017. 5467-5476.

[24] Bavirisetti DP, Dhuli R. Multi-focus image fusion using multi-scale image decomposition and saliency detection. Ain Shams Engineering Journal. 2018. 1103-17.

[25] Petsiuk V, Jain R, Manjunatha V, Morariu VI, Mehra A, Ordonez V, Saenko K. Black-box explanation of object detectors via saliency maps. In Proceedings of the IEEE/CVF Conference on Computer Vision and Pattern Recognition. 2021. 11443-11452.